ACS APPLIED MATERIALS & INTERFACES

Research Article

Cite This: ACS Appl. Mater. Interfaces 2018, 10, 32038−32046

www.acsami.org

Superwettable Microwell Arrays Constructed by Photocatalysis of Silver-Doped-ZnO Nanorods for Ultrasensitive and High-Throughput Electroanalysis of Glutathione in Hela Cells

Min Liu, Luping Feng, Xiaoyue Zhang, Yue Hua, Yuqi Wan, Chuan Fan, Xiaoxia Lv, and Hua Wang*

Institute of Medicine and Materials Applied Technologies, College of Chemistry and Chemical Engineering, Qufu Normal University, Qufu, Shandong 273165, P. R. China

Supporting Information

ABSTRACT: Superwettable microwell arrays were constructed for the first time by the synergic photocatalysis of silver-doped-ZnO (Ag−ZnO) nanorods patterned on indium tin oxide (ITO) electrodes for electroanalysis of glutathione (GSH) in hela cells through the signal output of AgCl electrochemistry. The newly prepared Ag−ZnO nanorods with high photocatalysis were dispersed into an octadecyltrichlorosilane (OTS) matrix to be deposited onto ITO substrates, yielding superhydrophobic Ag−ZnO−OTS coatings. Superhydrophilic microwells were further created by the Ag−ZnO photocatalysis under UV irradiation to produce Ag−ZnO microwell arrays featuring the superwettability profile. The resulting Ag−ZnO microwell-modified ITO electrodes were employed further for electroanalysis of GSH through solid-state AgCl electrochemistry, in which the specific Ag−GSH interactions would trigger a rational decrease in the sharp AgCl peak currents at the potential approaching zero. Moreover, benefitting from the superwettability feature, the microwells on the ITO electrodes could facilitate the condensing enrichment of GSH analytes from the sample droplets, achieving improved analysis sensitivity. The as-developed electroanalysis strategy was subsequently demonstrated for the detection of GSH in hela cell supernatant with levels down to about 27.30 pM. Additionally, this synergic photocatalysis-based preparation route can be tailored for the large-scale fabrication of various array platforms with the superwettability feature for high-throughput and sensitive biological analysis.

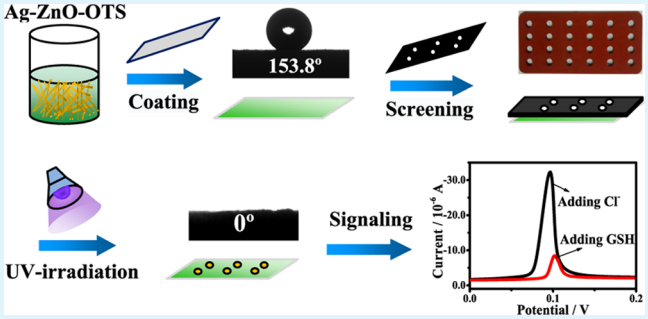

KEYWORDS: *microwell array, photocatalysis fabrication, silver-doped-ZnO nanorods, superwettable profile, glutathione electroanalysis*

INTRODUCTION

Glutathione (GSH) in human body plays a vital role in maintaining the biological functions.[1,2] It may serve as an antioxidant to remove excessive free radicals for protecting any cell damages.[3,4] Particularly, intracellular GSH is well recognized as an important clinical biomarker for the diagnosis of some serious diseases, such as liver damage, heart problems, and cancers.[5−7] To date, many analytical techniques have been developed for the evaluation of GSH, typically, such as the mass spectrometry,[8,9] high-performance liquid chromatography,[10,11] colorimetric test,[12,13] electrochemical analysis,[14,15] and fluorimetric techniques.[16,17] Among these detection methods, the electrochemical techniques may feature some unique advantages of cost effectiveness, rapid response, simple operation, and portability of devices.[18,19] Yet, the analysis performances of electrochemical assays largely depend on the electroactive signaling probes or functional interface materials modified on the electrodes. A variety of electroactive materials or labels have thus been fabricated and applied in the electrochemical sensing techniques.[20,21] As the most interesting representatives, noble metal nanomaterials like silver nanoparticles (AgNPs) have been employed as the electroactive probes for the design of various electrochemical sensors for detecting targets of biomedical importance[22−24] because AgNPs can present some advantages such as high electrocatalytic activity, cost effectiveness, and easy signal output.[25,26] Especially, the electroanalysis strategies by solid-state Ag/AgCl electrochemistry have been recognized to be advantageous over the conventional ones in terms of low redox potentials and large signal output with high sensing sensitivity.[22,24] For example, Zhang et al. developed an ultrasensitive DNA biosensor by the solid-state Ag/AgCl redox process.[22] An ultrasensitive electroanalysis method was also developed by our group for probing micro-RNAs by the amplified signal outputs of silver deposition.[24]

Received: August 4, 2018
Accepted: August 29, 2018
Published: August 30, 2018

DOI: 10.1021/acsami.8b13301
ACS Appl. Mater. Interfaces 2018, 10, 32038−32046

Scheme 1. Schematic Illustration of (A) the Fabrication Route of the Superwettable Ag−ZnO Microwell Array Created on the ITO Electrode Including the Superhydrophobic Coating with the Ag−ZnO−OTS mixture, Hole Making by Screening, and UV Irradiation-Induced Formation of Superhydrophilic Microwells, with the Changing Contact Angles (CAs); (B) the Formation Principle and Sensing Procedure of a Ag−ZnO Microwell Created on ITO for GSH Electroanalysis through the Electrochemical Output of Solid-State AgCl Signals, Where the Superhydrophobic Ag−ZnO−OTS Coating and UV Irradiation-Induced Formation of Superhydrophilic Ag−ZnO Microwells were Continuously Conducted on ITO to Interact First with Cl^- Ions and Then with GSH; (C) the Condensing Enrichment Process of Targeting GSH in the Droplet on the Ag−ZnO Microwell on the ITO Substrate

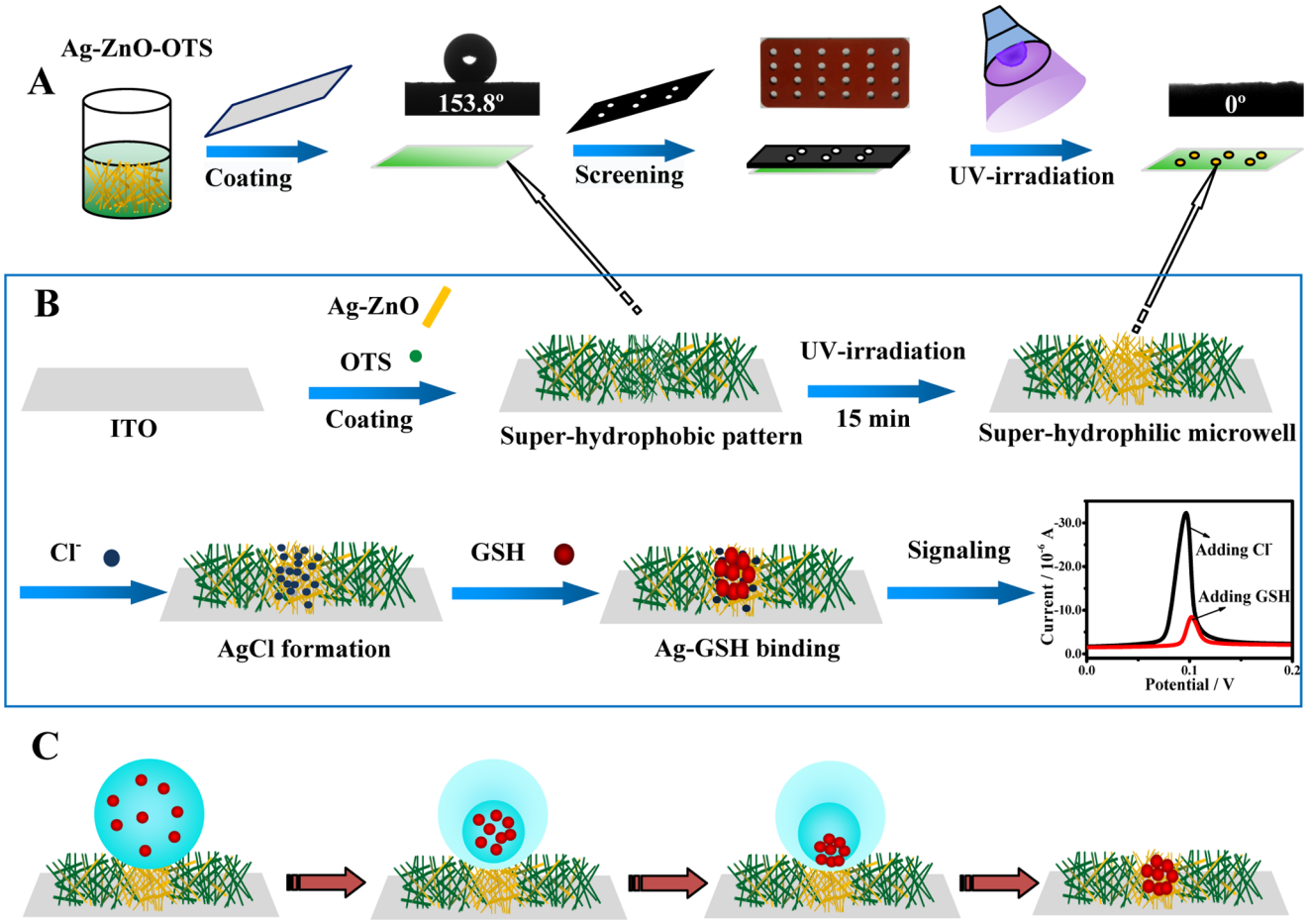

Because some meaningful levels of targeting biomarkers in cells may be considerably low at the early stage of diseases, the enrichment of the targets from the testing samples prior to the detections is highly desired. Recently, superhydrophobic surfaces have been employed for the design of sensing platforms for target enrichment,[27] in addition to the common applications for antifouling, oil−water separation, and self-cleaning.[28,29] It is well established that the contact area of a droplet on a superhydrophobic surface can be minimized, mostly known as the "lotus effect".[30,31] Because the sample droplets can possess small interfaces on a superhydrophobic substrate, the targets in the droplet may be enriched and concentrated into a small area, that is, the superhydrophobic surfaces may hold great potential for enriching targeting samples. For example, Wang et al. developed a unique sensing platform by spotting superhydrophilic microwells onto a superhydrophobic substrate for the target enrichment-based sensitive detection of nucleic acids.[27]

Recent decades have witnessed wide applications of photocatalytic materials of metal semiconductors such as ZnO because of their high physiochemical stability, low toxicity, and ease of availability.[32−34] However, ZnO photocatalysts may generally suffer from reduced photocatalytic efficiency under the UV−vis light due to the quick recombination of their photoexcited electrons and holes.[35] Alternatively, heterogeneous metal/semiconductor nanocomposites such as silver-doped ZnO nanocomposites have been utilized to expect increased photocatalytic efficiencies because silver can trap the photogenerated electrons from the semiconductors.[36−38] For example, Sun et al. fabricated Ag/ZnO nanocrystals with enhanced photocatalytic performances using glucose as a reducing agent.[39] Zhang and co-workers reported the controllable synthesis of hollow Ag−ZnO composites showing the increased photodegradation and electrocatalytic activities.[40]

Inspired by these pioneering discoveries, in the present work, Ag−ZnO nanorods with high photocatalysis were initially prepared and dispersed into an octadecyltrichlorosilane (OTS) matrix to be deposited onto the indium tin oxide (ITO) substrates to form superhydrophobic Ag−ZnO−OTS coatings. The photocatalytic creation of the superhydrophilic Ag−ZnO microwells was further performed under UV

DOI: 10.1021/acsami.8b13301
ACS Appl. Mater. Interfaces 2018, 10, 32038−32046

irradiation. The so-resulted Ag−ZnO microwells were discovered to display the superwettability feature so as to endow the as-modified ITO electrodes with condensing enrichment for GSH from sample droplets. Moreover, the as-prepared ITO electrodes were employed for electroanalysis of GSH through solid-state Ag/AgCl electrochemistry, in which the specific interactions of Ag atoms with sulfydryl-containing GSH[41] would trigger the rational decrease in the Ag/AgCl signals that can display a stable and sharp peak at the potential approaching zero. The photocatalysis-aided fabrication procedure of the Ag−ZnO microwell array on the ITO electrodes for GSH electroanalysis is schematically illustrated in Scheme 1, in which the microwell array on the ITO electrode could feature the superwettability profile for the condensing enrichment of analytes from the sample droplets. Remarkably, the superwettability profile of the microwell arrays developed in this article would aid to depress any crossover contamination of testing sample droplets,[42−44] so as to expect high-throughput and selective analysis of targeting GSH in hela cell supernatants. To the best of our knowledge, this is the first success of creating the superwettable microwell array onto the ITO electrodes by the synergic Ag−ZnO photocatalysis for ultrasensitive and high-throughput electroanalysis of low-level GSH through the signal output of solid-state AgCl electrochemistry.

EXPERIMENTAL SECTION

Reagents. Zinc acetate, oxalic acid, silver nitrate, and OTS were purchased from Sinopharm Chemical Reagent Co. (China). Phosphate-buffered saline (PBS) was obtained from Aladdin Reagent Co., Ltd. (Shanghai, China). Glutathione (GSH), valine (Val), threonine (Thr), lysine (Lys), leucine (Leu), trytophan (Try), phenylalanine (Phe), histidine (His), cysteine (Cys), ascorbic acid (AA), glucose (Glu), bovine serum albumin (BSA), and GSH assay kits were purchased from Sigma-Aldrich (Beijing, China). Hela cells were purchased from Shanghai SunBio Biomedical technology Co., Ltd. All other reagents were of analytical grade. Deionized water (>18 MΩ/cm) used was obtained from an ultrapure water system (Pall).

Apparatus. The prepared materials were characterized using scanning electron microscopy (SEM, Hitachi E-1010, Japan). The water contact angles were analyzed by the contact-angle measurement machine (Jinhe, Jiangsu, China). Electrochemical measurements were conducted using an electrochemical workstation CHI830 (CH Instrument, Shanghai, China) connected to a personal computer. A three-electrode system was applied consisting of an indium tin oxide (ITO, cut into 3 × 1.5 cm rectangular pieces) working electrode, a Pt wire counter electrode, and a Ag/AgCl reference electrode.

Synthesis of Photocatalytic Ag−ZnO Powders. Silver-doped ZnO (Ag−ZnO) nanocomposites were prepared according to a modified nonaqueous sol−gel synthesis and calcination route reported previously.[46] In a typical experiment, zinc acetate (2.19 g) and a certain amount of silver nitrate (0.051 g) were dissolved in ethanol (100 mL) and reflux-stirred at 60 °C for 30 min. Then, oxalic acid (2.51 g) dissolved in ethanol (40 mL) was introduced into the above mixture and was continuously reflux-stirred for 2.0 h at 60 °C. Afterward, the resulting thick white colloidal semigels were dried at 80 °C overnight in the dark. Subsequently, the dried products of Ag−ZnO powders were further calcined at 400 °C for 2.0 h and cooled down to room temperature to be stored in the dark for future use.

Preparation of the Ag−ZnO Microwell-Modified ITO Electrodes. The fabrication procedure of the Ag−ZnO microwell array is schematically illustrated in Scheme 1A. The ITO electrodes were first cleaned under UV light for 15 min. An aliquot of Ag−ZnO nanorods was dispersed into 1.0 mL of methylbenzene containing 10.0 μL of OTS to be sonicated for 2.0 min. Furthermore, 150 μL of the above mixture was dropped onto the surface of the ITO electrodes to be air-dried, yielding the superhydrophobic Ag−ZnO−OTS pattern. Then, a photomask with designed drill holes was utilized to cover the Ag−ZnO−OTS region on ITO electrodes and then aligned, clamped, and finally irradiated with a UV lamp for 15 min. The superhydrophilic Ag−ZnO microwell array was thereby created on the ITO electrodes with the superwettability profile.

Intracellular GSH Extraction from Hela Cells. The extraction of intracellular GSH from hela cells was performed according to the reported procedure.[45] Hela cell lines were incubated in DMEM containing glucose and fetal bovine serum (10.0%) in a humidified incubator (5.0% CO_2−95.0% air) at 37 °C. After being harvested through trypsinization, the cells were centrifuged (3000 rpm, 5 min), washed, and then re-dispersed in PBS solution. Furthermore, the cell lysates were obtained using an Radioimmunoprecipitation assay lysis buffer (100 μL) to be further centrifuged (12 000 rpm, 20 min). The intracellular GSH concentrations in the resulting samples of supernatants were determined according to the colorimetric instruction available in the GSH Assay Kit.

Ag−ZnO Microwell Array-Based Electroanalysis of GSH. Electrochemical measurements with the ITO electrodes modified with Ag−ZnO microwell arrays were performed in phosphate buffer (0.10 M, pH 7.4) containing Cl^- ions (40 mM) by the signal outputs of solid-state AgCl electrochemistry. Typically, an aliquot of GSH samples was separately introduced into the phosphate buffer above for the electrochemical measurements of linear sweep voltammetries (LSVs), which were performed in the potentials ranging from −0.20 to 0.40 V at a scanning speed of 100 mV/s. Moreover, the Ag−ZnO microwell-modified electrodes were used accordingly for the control tests for other ions and possibly interfering compounds including Ca^{2+}, K^+, Na^+, NH_4^+, Cl^-, Br^-, F^-, Val, Thr, Lys, Leu, Try, Phe, His, AA, Glu, and BSA, especially some common sulfides like S^{2-} and Cys as example.

Under the optimized detection conditions, the Ag−ZnO microwell-modified ITO electrodes were utilized to detect GSH with different concentrations in buffer (0.030−100.0 nM). Besides, the developed electroanalysis method was subsequently applied for the evaluation of intracellular GSH samples extracted from hela cells above.

RESULTS AND DISCUSSION

Fabrication Procedure and Sensing Principle of Ag−ZnO Microwell-Modified Electrodes for GSH Electroanalysis. It is well established that by doping silver into ZnO improved photocatalytic efficiency can be attained.[36−38] Herein, superwettable microwell arrays were constructed onto the ITO electrodes initially through the synergic Ag−ZnO photocatalysis under UV irradiation for GSH electroanalysis. Scheme 1 illustrates schematically the fabrication procedure and sensing principle for the microwell arrays created on the ITO electrode. As shown in Scheme 1A, Ag−ZnO nanorods, which were synthesized by a nonaqueous sol−gel synthesis and calcination route,[46] were dispersed into the OTS matrix to be further deposited onto the ITO substrate to yield the superhydrophobic Ag−ZnO−OTS pattern. Furthermore, UV irradiation was applied for the photocatalytic creation of the Ag−ZnO microwells using a photomask with the designed drill holes. It was found that the superhydrophobic pattern on the ITO substrate could present the average contact angle (CA) of about 153.8°. In contrast, the resulting irradiated region of microwells would display the average CA of about 0°, indicating the formation of superhydrophilic Ag−ZnO microwells. Notably, such a wettable profile of the microwell arrays could provide a lotuslike "self-cleaning" interface between the testing microwells so as to avoid any in-between fouling or crossover contamination of sample droplets.[42−44] As a result, the construction of denser microwell arrays could be expected for high-throughput and selective analysis of multiple analytes.

DOI: 10.1021/acsami.8b13301
ACS Appl. Mater. Interfaces 2018, 10, 32038−32046

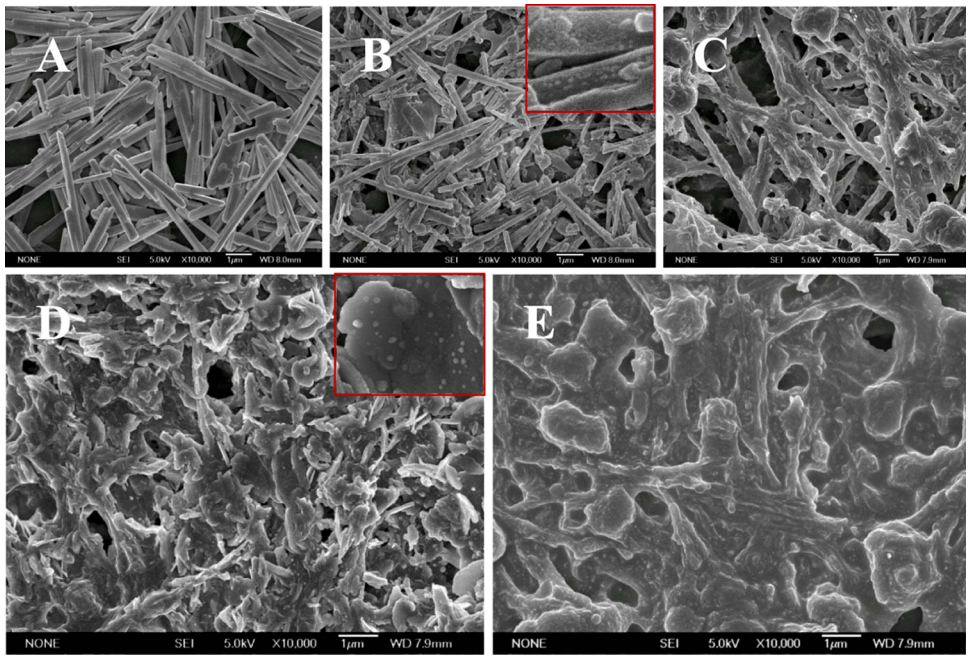

Figure 1. SEM images of the surfaces of ITO electrodes modified separately with (A) Ag−ZnO nanorods (the control), and Ag−ZnO−OTS (B) before (insert: the magnitude-amplified part) and (C) after UV irradiation to yield Ag−ZnO mcirowells, followed by the continuous additions of (D) Cl^- ions (insert: the magnitude-amplified part) and then (E) GSH.

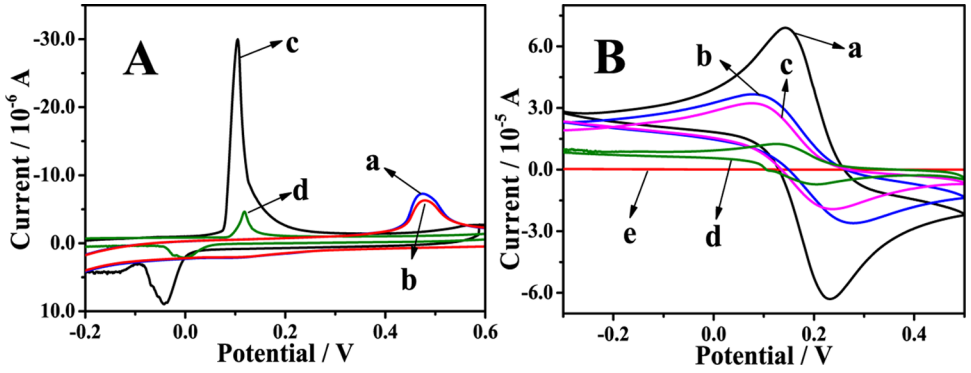

Figure 2. (A) Electrochemical CV responses of the Ag−ZnO microwell-modified electrodes to (a) blank, (b) GSH (no Cl^- ions), (c) Cl^- ions (40.0 mM), and then (d) GSH (25.0 nM). (B) Changing conductivities of the prepared electrodes in $K_3[Fe(CN)_6]$ (5.0 mM) during the step-by-step modification and sensing procedure of (a) bare and (b) Ag−ZnO microwells, followed by adding (c) Cl^- ions and then (d) GSH, taking (e) the Ag−ZnO−OTS-modified electrode without UV irradiation as the control.

Scheme 1B describes the formation and sensing procedures of a microwell modified on an ITO substrate, as an example, for GSH electroanalysis through the output of solid-state AgCl electrochemistry. One can note that under UV irradiation, the exposed region of OTS matrix coatings on Ag−ZnO nanorods could be dissolved photocatalytically so as to form superhydrophilic Ag−ZnO microwells on ITO substrate with the superhydrophobic pattern featuring superwettability. Furthermore, when Cl^- ions were introduced, the as-prepared ITO electrode would produce a stable and sharp AgCl peak at the potential approaching zero. Once GSH was added further, a ligand exchange between GSH and Cl^- ions would occur in the Ag−ZnO microwell because of the stronger Ag−GSH interaction.[41,45] As a result, a rational decrease in the AgCl signals was observed to facilitate electroanalysis of GSH. Moreover, Scheme 1C discloses the condensing enrichment process of a superhydrophilic microwell on the superhydrophobic substrate for concentrating the analytes from a sample droplet. Accordingly, the sensing signals of the as-prepared ITO electrode with the superwettable Ag−ZnO microwell array would be thus amplified toward the ultrasensitive GSH detections afterward.

The changing morphological structures of Ag−ZnO nanocomposites with the OTS matrix for creating microwells on ITO substrates were characterized by SEM imaging (Figure 1). It was observed that the original Ag−ZnO nanocomposites could display the uniform and well-defined rodlike structures (Figure 1A). After they were dispersed into the OTS matrix to be deposited onto ITO, a morphological composition of nanorods decorated with numerous particles was witnessed (Figure 1B), as more clearly shown in the amplified view (insert), showing the varying surface of the Ag−ZnO−OTS coating. Notably, the introduction of Ag−ZnO nanocomposites would additionally increase their surface roughness so as to improve the superhydrophobicity of the Ag−ZnO−OTS pattern, showing a CA of about 153.8° (Figure S1A).

DOI: 10.1021/acsami.8b13301
ACS Appl. Mater. Interfaces 2018, 10, 32038−32046

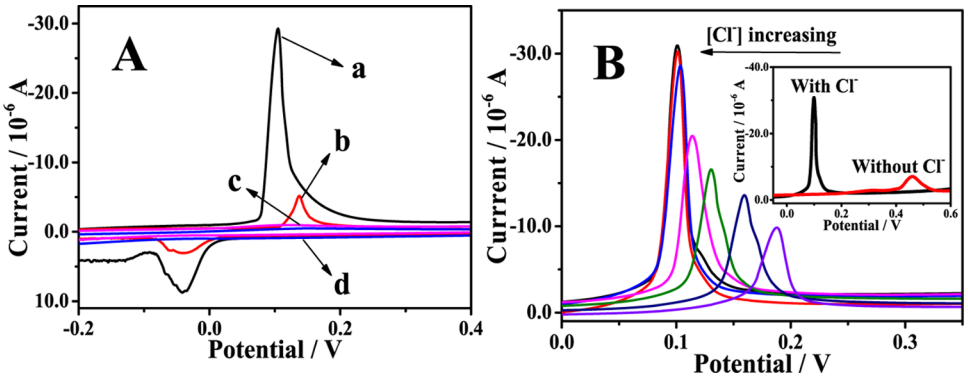

Figure 3. (A) Comparison of the electrochemical responses to Cl^- ions (40.0 mM) among the Ag−ZnO microwell-modified electrodes fabricated (a) with and (c) without UV irradiation, followed by adding GSH (b, d), respectively. (B) Effects of Cl^- amounts on the solid-state AgCl signals of Ag−ZnO microwell-modified electrodes (insert: comparison of the LSV responses between the as-modified electrodes with and without adding Cl^- ions). The electrochemical measurements were conducted using GSH (25.0 nM) at a sweep rate of 100 mV/s.

Interestingly, Figure 1C exhibits that the OTS particles on Ag−ZnO nanorods could be partly dissolved at the regions exposed to UV irradiation to attain superhydrophilicity with a CA approaching 0° (Figure S1B). Here, the hydrolysis reaction of trichlorosilane of OTS would take place by photocatalysis of Ag−ZnO nanorods under UV irradiation. Furthermore, upon adding Cl^- ions into the Ag−ZnO microwell, the nanorods could be mostly broken to yield the aggregation blocks decorated with some particles (Figure 1D), as clearly revealed by the amplified view (insert). Such a phenomenon might be presumably resulted from the interaction between Cl^- ions and the Ag element of Ag−ZnO nanorods, leading to AgCl precipitation. Yet, when GSH was introduced, a replacement reaction would occur between Cl^- ions and GSH to trigger the formation of aggregative fusions (Figure 1E).

Electrochemical Responses of the Ag−ZnO Microwell-Modified Electrodes for GSH. Electrochemical studies were conducted for the Ag−ZnO microwell-modified electrodes in sensing GSH through the solid-state Ag/AgCl electrochemistry (Figure 2). Figure 2A describes the cyclic voltammetry (CV) responses of the developed electrodes to Cl^- ions and then GSH. One can note that the as-prepared electrode could display only the silver oxidization peak at about 0.48 V in the absence of Cl^- ions (curve a). In contrast, the introduction of Cl^- ions could produce a couple of sharp oxidization and reduction peaks at the potentials of about 0.10 and −0.041 V, respectively, which are thus defined as the characteristic redox responses of solid-state Ag/AgCl (curve c). Herein, their current responses to GSH in the presence (curve d) of Cl^- ions could display a large difference at 0.10 V of the Ag/AgCl signal but showing no significant change at 0.48 V of silver oxidization in the absence of Cl^- ions (curve b). That is, a rational decrease of the solid-state AgCl signal could be specifically caused by GSH because of the stronger Ag−GSH interaction, thus achieving selective GSH electroanalysis. Figure 2B shows the changing conductivities of the Ag−ZnO microwell-modified electrodes during the step-by-step additions of first Cl^- and then GSH, by comparing with the bare electrode (curve a) and the one modified with superhydrophobic Ag−ZnO−OTS coating (without UV irradiation). As expected, the electrode modified with a superhydrophilic Ag−ZnO microwell could present a higher conductivity (curve b), which could be reduced after the addition of Cl^- ions (curve c) and especially GSH (curve d). In contrast, the electrode modified with the superhydrophobic coating could display no conductivity (curve e).

UV irradiation would play a vital role in the Ag−ZnO photocatalysis-based formation of Ag−ZnO microwells on the ITO electrodes. A comparison of electrochemical Cl^- responses between the electrodes patterned with the superhydrophobic Ag−ZnO−OTS coatings before and after UV irradiation is shown in Figure 3A. One can note that the electrode with the Ag−ZnO microwell formed after UV irradiation could produce a sharp peak of AgCl signal at about 0.10 V (curve a), which could disappear for the electrode fabricated without UV irradiation (curve c). Also, the addition of GSH would induce a large change of AgCl signal for the electrode with the Ag−ZnO microwell (curve b), whereas no significant change was obtained for the one created without UV irradiation (curve d). Therefore, UV irradiation would trigger the creation of superhydrophilic Ag−ZnO microwells on the ITO electrode, which could additionally expect the condensing enrichment of GSH from a sample droplet to realize the improved sensing responses.

Furthermore, the Cl^- effects on the electrochemical GSH responses were studied using the Ag−ZnO microwell-modified electrodes by the linear sweep voltammetry (LSV) output of solid-state AgCl signals (Figure 3B). It was discovered interestingly that the peak potentials of AgCl would decrease gradually approaching about 0.10 V as the Cl^- concentrations increased till 40 mM, over which equilibrium would reach. That is, the introduction of Cl^- ions would help achieve the sharp signals of solid-state AgCl at the desirably low peak potentials (i.e., 0.10 V), as opposed to the ones of silver oxidation (i.e., 0.48 V) (Figure 3B, insert). Therefore, the Ag−ZnO microwell-modified electrodes would promise the sensitive electroanalysis of GSH through the aforementioned solid-state AgCl electrochemistry.

Optimization of Electroanalysis Conditions of the Ag−ZnO Microwell-Modified Electrodes. The main conditions for GSH electroanalysis were optimized using the Ag−ZnO microwell-modified electrodes, with the results shown in Figure S2. It was found that the GSH responses could increase with increasing Ag in ZnO percentages until 6.0% (Figure S2A), which should be selected as the optimal one in the experiments. Moreover, the Ag−ZnO dosage-dependent responses to GSH were investigated (Figure S2B), showing the maximum current changes at 4.0 mg/mL of Ag−ZnO nanorods. Figure S2C shows the pH effects on the

DOI: 10.1021/acsami.8b13301
ACS Appl. Mater. Interfaces 2018, 10, 32038−32046

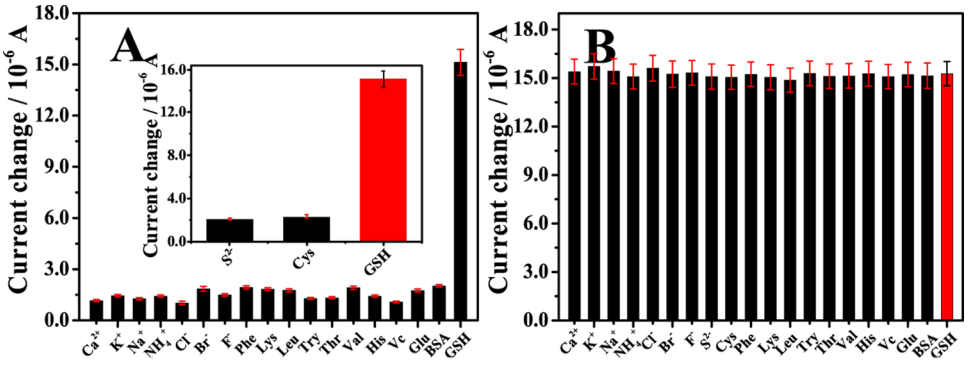

Figure 4. Electrochemical responses of solid-state AgCl signals of the Ag−ZnO microwell-modified electrodes to (A) different interferents (10.0 μM) alone (insert: comparable current changes among some common sulfides like S^{2-} ions and Cys with the same concentration) and (B) the interferents (10.0 μM) mixed separately with GSH (2.0 nM).

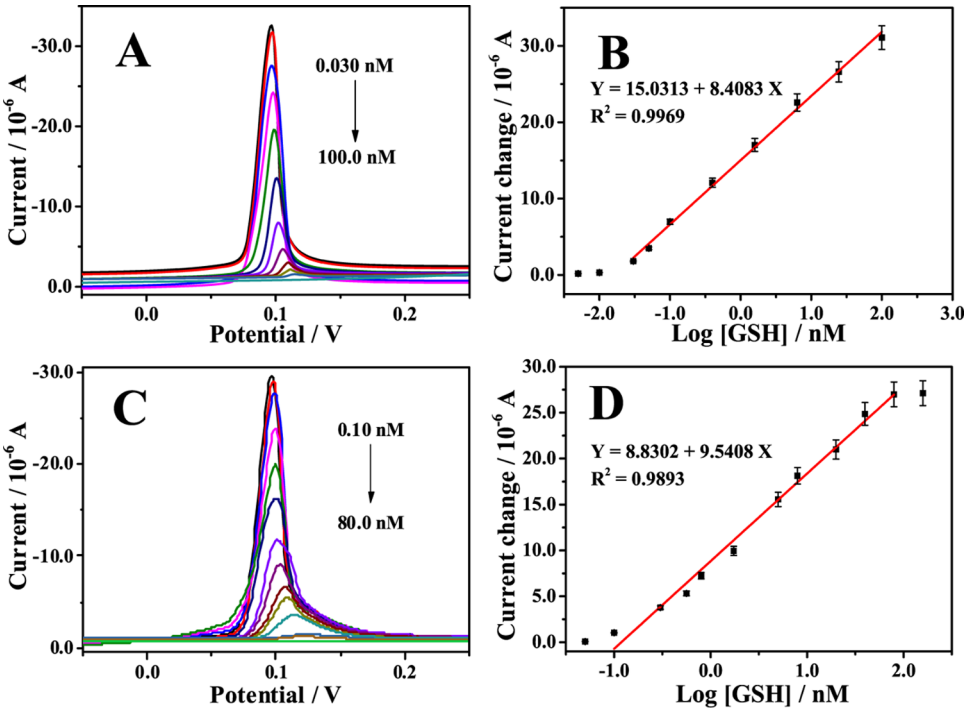

Figure 5. Electrochemical LSV responses of Ag−ZnO microwell-modified electrodes to GSH with different concentrations in (A) buffer and (C) cell supernatant at a sweep rate of 100 mV/s; (B, D) corresponding standard calibration curves describing the relationships between current responses and GSH concentrations, respectively.

electrochemical responses to GSH. Accordingly, the highest GSH-induced current changes could be obtained at pH 6.0 to be chosen as the optimal one. In addition, GSH electroanalysis was conducted with the Ag−ZnO microwell-modified electrodes under different ion strengths of NaCl concentrations (Figure S2D). To our surprise, the electrochemical responses of AgCl signals to GSH could be basically retained in the testing solutions containing NaCl up to 400 mM. Therefore, the developed Ag−ZnO microwell-modified electrodes could present a high environmental tolerance against harsh salinity, presumably resulting from the advantageous electrochemistry of solid-state AgCl.

Electroanalysis Performances of the Ag−ZnO Microwell-Modified Electrodes for GSH. The developed Ag−ZnO microwell-modified electrodes were employed for electroanalysis of GSH in comparison with some other ions and amino acids commonly coexisting in biological media (Figure 4). One can note that the tested ions and amino acids alone could present negligibly low responses even with higher concentrations (Figure 4A). Especially, some common sulfides like S^{2-} ions and cysteine (Cys) with the same concentration could display much lower responses (Figure 4A, insert), indicating that they might have no effect on GSH electroanalysis. Furthermore, Figure 4B manifests that when these testing substances were separately mixed with GSH, they still showed no significant effects on the GSH responses, as revealed by the data shown in Figure S3. Herein, the stronger Ag−GSH interaction would trigger the specific S−Cl replacement reactions, thus leading to a rational decrease of AgCl signals for sensing GSH. Highly selective GSH electroanalysis could thereby be expected to show the desirable detection performance against any interference for probing GSH in some complicated samples such as cell supernatant afterward. Moreover, the electroanalysis reproducibility of the developed ITO electrodes was explored in ten repeated experiments of GSH detections, displaying basically similar

DOI: 10.1021/acsami.8b13301
ACS Appl. Mater. Interfaces 2018, 10, 32038−32046

responses to GSH (Figure S4A). In addition, the sensing stability of the as-prepared electrodes was investigated (Figure S4B). As expected, the current responses to GSH might show no significant change even if the Ag−ZnO microwell-modified electrodes were stored for twelve months. These results indicate that the electrodes developed by the electroanalysis method can possess favorably high stability and reproducibility for the detection of GSH.

Ag−ZnO Microwell-Based Electroanalysis of GSH. Under the optimized analysis conditions, the Ag−ZnO microwell-modified electrodes were utilized to detect GSH of different concentrations separately in buffer and hela cell supernatant (Figure 5). As shown in Figure 5A, the current responses of the Ag−ZnO microwell-modified electrodes could decrease with increasing GSH concentrations. A linear relationship was thus obtained for the electrochemical responses over GSH concentrations ranging from 0.030 to 100.0 nM (Figure 5B), with the limit of detection (LOD) of about 11.25 pM, estimated by the 3 σ rule. Subsequently, the application feasibility of the so-established electroanalysis strategy was explored for the detection of intracellular GSH in the hela cell supernatant, of which the initial GSH concentrations were determined by the GSH assay kit. The current responses of the developed electrodes were recorded for different diluted GSH concentrations (Figure 5C). Figure 5D describes that GSH in cell supernatant could be detected with the concentrations linearly ranging from 0.10 to 80.0 nM, with the LOD of 27.30 pM. In addition, the advantages of the developed electroanalysis strategy were investigated by comparing with other electroanalysis methods documented for GSH detections, with the results summarized in Table S1. Accordingly, the developed electroanalysis method can present better detection performances in terms of LODs and thus promising for the extensive practical applications for the analysis of GSH in biological media like cancer cell supernatant.

CONCLUSIONS

In summary, superwettable Ag−ZnO microwell arrays were successfully created onto the ITO electrodes initially by photocatalysis of Ag−ZnO nanorods under UV irradiation. The resulting Ag−ZnO microwell-modified electrodes were further employed for high-throughput electroanalysis of GSH by the signal outputs of solid-state AgCl electrochemistry. The developed electroanalysis strategy possesses some outstanding advantages over the current analyses for GSH using other kinds of sensing platforms or electroactive probes. First, Ag−ZnO microwell array could be fabricated on a large scale on ITO electrodes simply by photocatalysis of Ag−ZnO nanorods newly prepared, in which the doping of Ag element would endow ZnO with stronger photocatalysis. Second, stable and sharp electrochemical peaks of solid-state AgCl could be obtained for the Ag−ZnO microwell-modified electrodes at a considerably low potential approaching zero so as to circumvent any redox interference from possibly coexisting electroactive substances in the background. Third, the powerful Ag−GSH interactions could trigger the specific S−Cl replacement reactions, leading to the rational decrease of AgCl signals and facilitating the direct detection of GSH in hela cells with high detection selectivity and sensitivity. Finally, the so-yielded Ag−ZnO microwell array with the superwettability feature could enjoy the condensing enrichment of analytes (i.e., GSH) from the sample droplets so as to achieve more sensitive responses. Especially, it would help to avoid any possible crossover contamination between the sample droplets on the microwell arrays for high-throughput analysis of different targets. Therefore, the developed ultrasensitive and high-throughput electroanalysis sensor may find field-deployable applications for probing the low-level GSH in various biological media (i.e., cell supernatant) for the early warning or diagnosis of clinically serious diseases like cancers. In particular, such a microwell preparation route by the synergic Ag−ZnO photocatalysis would open a new door toward the large-scale fabrication of a variety of functional microarrays, whose superwettability feature would promise high-throughput and sensitive biological analysis.

ASSOCIATED CONTENT

Supporting Information

The Supporting Information is available free of charge on the ACS Publications website at DOI: 10.1021/acsami.8b13301.

Additional results for the characterization of contact angle Ag−ZnO−OTS before and after UV irradiation; the optimization of electroanalysis conditions including Ag in ZnO percentages, Ag−ZnO concentrations, pH values, and NaCl concentrations; the electroanalysis selectivity, GSH sensing reproducibility and stability; and comparison of analytical results among different documented methods (PDF)

AUTHOR INFORMATION

Corresponding Author

*E-mail: huawangqfnu@126.com. Tel: +86 537 4456306. Web: http://wang.qfnu.edu.cn.

ORCID

Hua Wang: 0000-0003-0728-8986

Author Contributions

All authors have given approval to the final version of the manuscript.

Notes

The authors declare no competing financial interest.

ACKNOWLEDGMENTS

This work is supported by the National Natural Science Foundations of China (Nos. 21675099, 21375075, and 21601106) and the Major Basic Research Program of Natural Science Foundation of Shandong Province, P. R. China (ZR2018ZC0129).

REFERENCES

(1) Sekhar, R. V.; McKay, S. V.; Patel, S. G.; Guthikonda, A. P.; Reddy, V. T.; Balasubramanyam, A.; Jahoor, F. Glutathione Synthesis is Diminished in Patients with Uncontrolled Diabetes and Restored by Dietary Supplementation with Cysteine and Glycine. *Diabetes Care* **2011**, *34*, 162−167.

(2) Yu, F.; Li, P.; Wang, B.; Han, K. Reversible Near-infrared Fluorescent Probe Introducing Tellurium to Mimetic Glutathione Peroxidase for Monitoring the Redox Cycles between Peroxynitrite and Glutathione in Vivo. *J. Am. Chem. Soc.* **2013**, *135*, 7674−7680.

(3) Raj, L.; Ide, T.; Gurkar, A. U.; Foley, M.; Schenone, M.; Li, X.; Tolliday, N. J.; Golub, T. R.; Carr, S. A.; Shamji, A. F.; Stern, A. M.; Mandinova, A.; Schreiber, S. L.; Lee, S. W. Selective Killing of Cancer Cells by a Small Molecule Targeting the Stress Response to ROS. *Nature* **2012**, *481*, 534.

(4) Carocho, M.; Ferreira, I. C. A Review on Antioxidants, Prooxidants and Related Controversy: Natural and Synthetic

DOI: 10.1021/acsami.8b13301
ACS Appl. Mater. Interfaces 2018, 10, 32038−32046

Compounds, Screening and Analysis Methodologies and Future Perspectives. *Food Chem. Toxicol.* **2013**, *51*, 15−25.
(5) Li, J.; Shu, Y.; Hao, T.; Wang, Y.; Qian, Y.; Duan, C.; Sun, H.; Lin, Q.; Wang, C. A Chitosan-glutathione Based Injectable Hydrogel for Suppression of Oxidative Stress Damage in Cardiomyocytes. *Biomaterials* **2013**, *34*, 9071−9081.
(6) Ortega, A. L.; Mena, S.; Estrela, J. M. Glutathione in Cancer Cell Death. *Cancers* **2011**, *3*, 1285−1310.
(7) Zhu, R.; Wang, Y.; Zhang, L.; Guo, Q. Oxidative Stress and Liver Disease. *Hepatol. Res.* **2012**, *42*, 741−749.
(8) Squellerio, I.; Caruso, D.; Porro, B.; Veglia, F.; Tremoli, E.; Cavalca, V. Direct Glutathione Quantification in Human Blood by LC-MS/MS: Comparison with HPLC with Electrochemical Detection. *J. Pharm. Biomed. Anal.* **2012**, *71*, 111−118.
(9) Chiang, C. K.; Chen, W. T.; Chang, H. T. Nanoparticle-based Mass Spectrometry for the Analysis of Biomolecules. *Chem. Soc. Rev.* **2011**, *40*, 1269−1281.
(10) Marchand, S.; de Revel, G. A HPLC Fluorescence-based Method for Glutathione Derivatives Quantification in Must and Wine. *Anal. Chim. Acta* **2010**, *660*, 158−163.
(11) Mcdermott, G. P.; Francis, P. S.; Holt, K. J.; Scott, K. L.; Martin, S. D.; Stupka, N.; Barnett, N. W.; Conlan, X. A. Determination of Intracellular Glutathione and Glutathione Disulfide Using High Performance Liquid Chromatography with Acidic Potassium Permanganate Chemiluminescence Detection. *Analyst* **2011**, *136*, 2578−2585.
(12) Li, Y.; Wu, P.; Xu, H.; Zhang, H.; Zhong, X. Anti-aggregation of Gold Nanoparticle-based Colorimetric Sensor for Glutathione with Excellent Selectivity and Sensitivity. *Analyst* **2011**, *136*, 196−200.
(13) Jung, H. S.; Chen, X.; Kim, J. S.; Yoon, J. Recent Progress in Luminescent and Colorimetric Chemosensors for Detection of Thiols. *Chem. Soc. Rev.* **2013**, *42*, 6019−6031.
(14) Pacsial-Ong, E. J.; McCarley, R. L.; Wang, W.; Strongin, R. M. Electrochemical Detection of Glutathione Using Redox Indicators. *Anal. Chem.* **2006**, *78*, 7577−7581.
(15) Wang, Z.; Han, P.; Mao, X.; Yin, Y.; Cao, Y. Sensitive Detection of Glutathione by Using DNA-templated Copper Nanoparticles as Electrochemical Reporters. *Sens. Actuators, B* **2017**, *238*, 325−330.
(16) Gu, J.; Hu, D.; Wang, W.; Zhang, Q.; Meng, Z.; Jia, X.; Xi, K. Carbon Dot Cluster as an Efficient "Off-on" Fluorescent Probe to Detect Au (III) and Glutathione. *Biosens. Bioelectron.* **2015**, *68*, 27−33.
(17) Liu, J.; Bao, C.; Zhong, X.; Zhao, C.; Zhu, L. Highly Selective Detection of Glutathione Using a Quantum-dot-based Off-on Fluorescent Probe. *Chem. Commun.* **2010**, *46*, 2971−2973.
(18) Miao, P.; Liu, L.; Nie, Y.; Li, G. An Electrochemical Sensing Strategy for Ultrasensitive Detection of Glutathione by Using Two Gold Electrodes and Two Complementary Oligonucleotides. *Biosens. Bioelectron.* **2009**, *24*, 3347−3351.
(19) Shahmiri, M. R.; Bahari, A.; Karimi-Maleh, H.; Hosseinzadeh, R.; Mirnia, N. Ethynylferrocene-NiO/MWCNT Nanocomposite Modified Carbon Paste Electrode as a Novel Voltammetric Sensor for Simultaneous Determination of Glutathione and Acetaminophen. *Sens. Actuators, B* **2013**, *177*, 70−77.
(20) Lai, W.; Zhuang, J.; Tang, J.; Chen, G.; Tang, D. One-step Electrochemical Immunosensing for Simultaneous Detection of Two Biomarkers Using Thionine and Ferrocene as Distinguishable Signal Tags. *Microchim. Acta* **2012**, *178*, 357−365.
(21) Tan, Y.; Qiu, J.; Cui, M.; Wei, X.; Zhao, M.; Qiu, B.; Chen, G. An Immobilization Free DNAzyme Based Electrochemical Biosensor for Lead Determination. *Analyst* **2016**, *141*, 1121−1126.
(22) Zhang, J.; Ting, B. P.; Jana, N. R.; Gao, Z.; Ying, J. Y. Ultrasensitive Electrochemical DNA Biosensors Based on the Detection of a Highly Characteristic Solid-state Process. *Small* **2009**, *5*, 1414−1417.
(23) Liu, M.; Zhang, L. Y.; Hua, Y.; Feng, L. P.; Jiang, Y.; Ding, X. J.; Qi, W.; Wang, H. Mesoporous Silver-melamine Nanowires Formed by Controlled Supermolecular Self-Assembly: A Selective Solid-state Electroanalysis for Probing Multiple Sulfides in Hyperhaline Media through the Specific Sulfide-chloride Replacement Reactions. *Anal. Chem.* **2017**, *89*, 9552−9558.
(24) Si, Y.; Sun, Z. Z.; Zhang, N.; Qi, W.; Li, S. Y.; Chen, L. J.; Wang, H. Ultrasensitive Electroanalysis of Low-level Free MicroRNAs in Blood by Maximum Signal Amplification of Catalytic Silver Deposition Using Alkaline Phosphatase-incorporated Gold Nanoclusters. *Anal. Chem.* **2014**, *86*, 10406−10414.
(25) Miao, P.; Wang, B.; Yin, J.; Chen, X.; Tang, Y. Electrochemical Tracking Hydrogen Peroxide Secretion in Live Cells Based on Autocatalytic Oxidation Reaction of Silver Nanoparticles. *Electrochem. Commun.* **2015**, *53*, 37−40.
(26) Miao, P.; Meng, F.; Wang, B.; Zhu, X.; Tang, Y. Highly Sensitive MicroRNA Quantification with Zero Background Signal from Silver Nanoparticles. *Electrochem. Commun.* **2015**, *51*, 89−92.
(27) Xu, L. P.; Chen, Y.; Yang, G.; Shi, W.; Dai, B.; Li, G.; Cao, Y.; Wen, Y.; Zhang, X.; Wang, S. Ultratrace DNA Detection Based on the Condensing-enrichment Effect of Superwettable Microchips. *Adv. Mater.* **2015**, *27*, 6878−6884.
(28) Zhang, W.; Shi, Z.; Zhang, F.; Liu, X.; Jin, J.; Jiang, L. Superhydrophobic and Superoleophilic PVDF Membranes for Effective Separation of Water-in-oil Emulsions with High Flux. *Adv. Mater.* **2013**, *25*, 2071−2076.
(29) Su, B.; Wang, S.; Wu, Y.; Chen, X.; Song, Y.; Jiang, L. Small Molecular Nanowire Arrays Assisted by Superhydrophobic Pillar-Structured Surfaces with High Adhesion. *Adv. Mater.* **2012**, *24*, 2780−2785.
(30) Feng, X.; Zhai, J.; Jiang, L. The Fabrication and Switchable Superhydrophobicity of TiO_2 Nanorod Films. *Angew. Chem., Int. Ed.* **2005**, *44*, 5115−5118.
(31) Wang, S.; Feng, X.; Yao, J.; Jiang, L. Controlling Wettability and Photochromism in a Dual-responsive Tungsten Oxide Film. *Angew. Chem., Int. Ed.* **2006**, *45*, 1264−1267.
(32) Vayssieres, L. Growth of Arrayed Nanorods and Nanowires of ZnO from Aqueous Solutions. *Adv. Mater.* **2003**, *15*, 464−466.
(33) Hoffmann, M. R.; Martin, S. T.; Choi, W.; Bahnemann, D. W. Environmental Applications of Semiconductor Photocatalysis. *Chem. Rev.* **1995**, *95*, 69−96.
(34) Afzaal, M.; Malik, M. A.; O'Brien, P. Preparation of Zinc Containing Materials. *New J. Chem.* **2007**, *31*, 2029−2040.
(35) Huang, Q.; Zhang, Q.; Yuan, S.; Zhang, Y.; Zhang, M. One-pot Facile Synthesis of Branched Ag−ZnO Heterojunction Nanostructure as Highly Efficient Photocatalytic Catalyst. *Appl. Surf. Sci.* **2015**, *353*, 949−957.
(36) Sun, S.; Wang, W.; Zeng, S.; Shang, M.; Zhang, L. Preparation of Ordered Mesoporous Ag/WO_3 and its Highly Efficient Degradation of Acetaldehyde under Visible-light Irradiation. *J. Hazard. Mater.* **2010**, *178*, 427−433.
(37) Liu, Y.; Wei, S.; Gao, W. Ag/ZnO Heterostructures and their Photocatalytic Activity under Visible Light: Effect of Reducing Medium. *J. Hazard. Mater.* **2015**, *287*, 59−68.
(38) Wang, R.; Xin, J. H.; Yang, Y.; Liu, H.; Xu, L.; Hu, J. The Characteristics and Photocatalytic Activities of Silver Doped ZnO Nanocrystallites. *Appl. Surf. Sci.* **2004**, *227*, 312−317.
(39) Sun, F.; Tan, F.; Wang, W.; Qiao, X.; Qiu, X. Facile Synthesis of Ag/ZnO Heterostructure Nanocrystals with Enhanced Photocatalytic Performance. *Mater. Res. Bull.* **2012**, *47*, 3357−3361.
(40) Zhang, D.; Li, J.; Chen, Y.; Wu, Q.-S.; Ding, Y.-P. One-pot Preparation and Enhanced Photocatalytic and Electrocatalytic Activities of Ultralarge Ag/ZnO Hollow Coupled Structures. *CrystEngComm* **2012**, *14*, 6738−6743.
(41) Liu, C.; Zheng, J.; Deng, L.; Ma, C.; Li, J.; Li, Y.; Yang, S.; Yang, J.; Wang, J.; Yang, R. Targeted Intracellular Controlled Drug Delivery and Tumor Therapy through in Situ Forming Ag Nanogates on Mesoporous Silica Nanocontainers. *ACS Appl. Mater. Interfaces* **2015**, *7*, 11930−11938.
(42) Li, S. Y.; Dong, M. M.; Li, R.; Zhang, L. Y.; Qiao, Y. C.; Jiang, Y.; Qi, W.; Wang, H. A Fluorometric Microarray with ZnO Substrate-enhanced Fluorescence and Suppressed "Coffee-ring" Effects for Fluorescence Immunoassays. *Nanoscale* **2015**, *7*, 18453−18458.

DOI: 10.1021/acsami.8b13301
ACS Appl. Mater. Interfaces 2018, 10, 32038−32046

(43) Feng, L.; Liu, M.; Liu, H.; Fan, C.; Cai, Y. Y.; Chen, L. J.; Zhao, M. L.; Chu, S.; Wang, H. High-Throughput and Sensitive Fluorimetric Strategy for MicroRNAs in Blood Using Wettable Microwells Array and Silver Nanoclusters with Red Fluorescence Enhanced by Metal Organic Frameworks. *ACS Appl. Mater. Interfaces* **2018**, *10*, 23647−23656.
(44) Li, S. Y.; Li, R.; Dong, M. M.; Zhang, L. Y.; Jiang, Y.; Chen, L. J.; Qi, W.; Wang, H. High-Throughput, Selective, and Sensitive Colorimetry for Free MicroRNAs in Blood via Exonuclease I Digestion and Hemin-G-Quadruplex Catalysis Reactions Based on a "Self-Cleaning" Functionalized Microarray. *Sens. Actuators, B* **2015**, *222*, 198−204.
(45) Lv, Y.; Lu, M.; Yang, Y.; Yin, Y.; Zhao, J. Electrochemical Detection of Intracellular Glutathione Based on Ligand Exchange Assisted Release of DNA-templated Silver Nanoparticles. *Sens. Actuators, B* **2017**, *244*, 151−156.
(46) Georgekutty, R.; Seery, M. K.; Pillai, S. C. A Highly Efficient Ag−ZnO Photocatalyst: Synthesis, Properties, and Mechanism. *J. Phys. Chem. C* **2008**, *112*, 13563−13570.

DOI: 10.1021/acsami.8b13301
ACS Appl. Mater. Interfaces 2018, 10, 32038−32046